J. Univ. Kuwait (Sci.) **11**, 1984

Application of hard magnetic materials to improve performance of electric machines

M. H. SALAMA

Department of Electrical Engineering, University of Kuwait

ABSTRACT

The hard magnetic materials which exhibit high values of hysteresis loss per cycle can be represented by equivalent electric parameters. When introduced into the secondary circuit of an induction motor, these parameters will result in improving the starting performance of this motor. A digital computer program has been built to simulate a model for the hard magnetic material when inserted inside the rotor slots of a squirrel cage induction motor and to study their effect on the steady-state performance of the motor.

INTRODUCTION

The importance of using permanent magnetic materials, based on aluminium–nickel–iron alloys, in electric machines has been widely recognized for some time (Alger *et al.* 1963; Gunn 1963; Dubey & De 1973; Sabir *et al.* 1975). Such materials, known as hard magnetic materials, have been found to exhibit high values of hysteresis loss per cycle, coercive force and residual induction (Hick 1974). Alger *et al.* (1963) utilised these features and selected Alnico V for the construction of a saturistor. The saturistor, which is a coil with a hard magnet as a core was then designed and connected to the rotor terminals to improve the starting performance of the slip ring induction motor. To study the behaviour of saturistors when used with motors, Sabir & Shepherd (1974) and Shepherd *et al.* (1974) investigated thoroughly the properties of Alcomax III when subjected to a variety of working conditions.

All the previous investigations dealt with saturistor reactors which were connected externally to the rotor terminals via slip rings. However, the present work applies the saturistor material inside the rotor of a squirrel cage motor so that no slip rings or external connections are required. This paper deals with Alcomax III when inserted in the slots of the cage of a squirrel cage induction motor. By these arrangements a saturistor can be built inside the rotor but with one turn coil which is the copper bar sharing the same slot. As a result, additional rotor resistance due to the high hysteresis loss in the hard magnet is shown to improve the motor starting performance. A computer program has been built to simulate the squirrel cage induction motor with Alcomax III inserted above the copper bars of the rotor. The program consists of two stages. In the first stage the electrical equivalent circuit of Alcomax III bars when a

current passes through the copper bars of the rotor is computed. In the second stage the motor steady-state performance is computed.

EVALUATION OF THE EQUIVALENT CIRCUIT OF A COIL-WOUND SATURISTOR

To study the validity of the method suggested for the evaluation of an equivalent circuit of Alcomax III bar when inserted above the copper conductor in a slot, a coil-wound saturistor will be considered first. A coil-wound saturistor is made of a hard magnetic core around which a number of turns are wound. When this saturistor is connected to a sinusoidal voltage source, it is usually assumed that the resulting flux varies sinusoidally with time. By considering the geometrical notation of the saturistor core shown in Fig. 1, the maximum flux density B_x can be readily calculated. The static

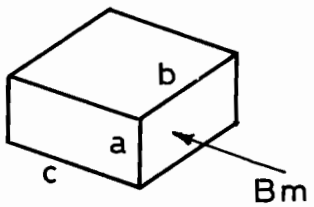

Fig. 1. The geometrical notation of the sample.

B–H loops for the hard magnetic material will then be used to evaluate the associated magnetising force H_x. From Ampere's law,

$$\oint H_x \, \mathrm{dl} = N I \tag{1}$$

the magnetising current I can be calculated. Since the magnetising current is almost a square wave (Alger 1965), the root mean square value is approximately equal to the peak value.

The area within the static B–H loop bounded by B_x and H_x, is equal to the hysteresis loss per unit volume per cycle, p_ℓ, under cyclic excitation provided that the eddy current and anomalous losses are negligible. The total hysteresis loss P_L is given by

$$\begin{aligned} P_L &= p\ell \times \text{volume} \times \text{frequency} \\ &= p\ell \times (a\ b\ c) \times f \\ &= I^2 R_s \end{aligned} \tag{2}$$

where R_s is the equivalent resistance representing hysteresis loss developed by the saturistor core at B_x.

The equivalent impedance of the saturistor core at B_x is defined by

$$\begin{aligned} Z_s &= \frac{V_{\text{rms}}}{I} = \frac{4{\cdot}44\ \phi f}{I} \\ &= \frac{4{\cdot}44\ B_x a\ b\ f}{I} \end{aligned} \tag{3}$$

This would only be true if both the current and voltage are sinusoidal. Adding the exciting coil parameters R_c & X_c, the equivalent electrical parameters of a coil-wound saturistor will be

$$R_T = R_c + R_s \tag{4}$$

$$X_T = X_c + X_s \tag{5}$$

$$Z_T^2 = R_T^2 + X_T^2 \quad . \tag{6}$$

The previous procedure was tested by comparing the equivalent circuit parameters using the static B–H curves with that obtained from experimental results carried out by other investigators (Alger *et al.* 1963; Alger 1965). The results are presented in Table 1.

Table 1. Comparison of calculated parameters and tested results obtained by Alger *et al.* (1963) and Alger (1965)

	Calculated from theory			Tested*		Correction factors	
Exciting current I(Amp)	R_T	Z_T	X_T	R_A	Z_A	$K_a = \frac{Z_A}{Z_T}$	$H_a = \frac{R_a}{R_T}$
43·8	0·652	1·280	1·110	0·730	1·020	0·790	1·070
45·8	0·820	1·490	1·214	0·810	1·077	0·723	0·988
48·0	0·857	1·628	1·317	0·877	1·200	0·737	1·035
61·8	0·710	1·517	0·343	0·830	0·277	0·842	1·169
156·0	0·206	0·894	0·870	0·246	0·740	0·828	1·194

* References: Alger *et al.* (1963) and Alger (1965).

DISCUSSION OF THE RESULTS

(i) In general, there is good agreement between the measured and calculated variations of R and Z with H over a wide range.

(ii) The measured impedance is less than the calculated value by about 20%. This may be due to the approximated wave forms assumed for both voltage and current.

(iii) At low range of the exciting current, the error between measured and calculated resistances can be tolerated. For high values of exciting current, higher measured values of resistance may be due to the effect of additional losses introduced by the yoke used.

EFFECT OF EDDY CURRENTS IN THE SATURISTOR

Under conditions of *ac* excitation, induced eddy currents may modify the electrical equivalent circuit of a coil-wound saturistor. Experimental data related to this effect have been published (Sabir & Shepherd 1974; Shepherd *et al.* 1974) from which the following observations are made:

(i) Eddy currents cause the dynamic B–H loops to be shorter and wider than the static loops.

(ii) For a given H, the values of maximum flux density and residual flux density are generally reduced. This in turn reduces the measured values of Z and consequently the ratio K_a will be less than unity.

(iii) For low H, the dynamic power loss is less than that obtained from the static B–H loop. At high H, the loss is higher than that given by the static loop.

(iv) Sabir & Shepherd (1974) have presented measurements at frequencies greater than 50 Hz from which it is noted that the eddy current has contributed to the iron loss a percentage value of 8% and 21% of the total losses at 50 and 300 Hz, respectively.

However, eddy current losses depend not only on frequency but also on the dimensions of the core. It is well known that the theoretical eddy current loss is given by

$$P_e = \frac{a^3}{24\rho} \mathrm{B}_x^2 (2\pi f)^2 bc \text{ watt} \quad . \tag{7}$$

It was noticed that both the dimensions (a, b and c) of the test samples and the supply frequency used by other investigators are different. So, by assuming the flux density B_x to be the same, the quantity ($a^3\, bc\, f^2$) is singled out and presented in Table 2 for the purpose of allowing relative levels of eddy current losses to be compared between samples used by different investigators and the sample under test. The supply frequency used in the present study is 400 Hz.

It is clear from the results shown in Table 2 that the eddy current losses in the suggested test sample is very much less than those occurring in most of the saturistors referred to in the literature. The high values of the quantity ($a^3\, bc\, f^2$) presented by the different test samples, support the discrepancies between tested and calculated results presented in the corresponding papers. Although the sample nearest in size and frequency to the test sample is that used by Sabir & Shepherd (350 Hz), the quantity indicates a loss in the range of 14 times. It can be concluded that the eddy current losses

Table 2. Eddy loss values for different hard magnetic materials

Sample (i.e. reference)	Dimension of sample used in cm			Material of sample	Frequency of source used (f) Hz	The quantity ($a^3 bc f^2$)
	a	b	c			
Gunn (1963)	3·81	15·24	3·81	Alnico V	60	$11{\cdot}50 \times 10^6$
Gunn (1963)	2·86	10·16	3·81	Alnico V	60	$3{\cdot}27 \times 10^6$
Alger (1965)	2·54	9·53	7·62	Alcomax III	60	$4{\cdot}30 \times 10^6$
Sabir & Shepherd (1974)	2·50	2·50	4·00	Alcomax III	50	$3{\cdot}90 \times 10^5$
Sabir & Shepherd (1974)	1·00	1·00	4·00	Alcomax III	50	$1{\cdot}00 \times 10^4$
Sabir & Shepherd (1974)	0·56	1·25	4·00	Alcomax III	350	$7{\cdot}68 \times 10^4$
Shepherd *et al.* (1974) (max. size)	2·50	2·50	4·00	Alcomax III	50	$3{\cdot}90 \times 10^4$
Shepherd *et al.* (1974) (min. size)	1·00	1·00	4·00	Alcomax III	50	$1{\cdot}00 \times 10^4$
Sample under test	0·20	11·43	0·26	Alcomax III	400	$4{\cdot}00 \times 10^3$

for the test sample under investigation will hardly affect the computed performance and then can be neglected.

EQUIVALENT ELECTRIC CIRCUIT OF A MODIFIED SQUIRREL CAGE MOTOR

The slot of an ordinary squirrel cage rotor will now be modified to allow for the insertion of a cast hard magnetic bar on top of the copper bar. The hard magnetic material used in this investigation is Alcomax III. Fig. 2 illustrates the assumed arrangement inside a rotor slot where w_s is the width of the saturistor bar used and w_a represents the total sum of air gaps between saturistor bar and the side walls of the slot.

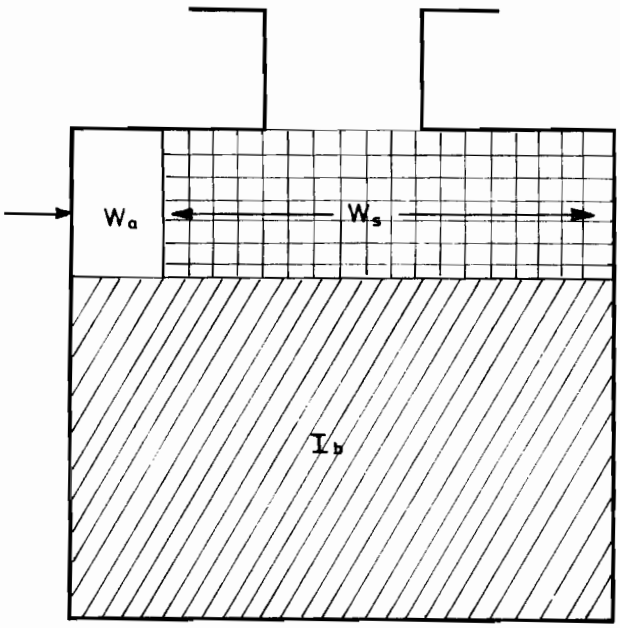

Fig. 2. The arrangement inside a rotor slot.

The previous procedure used for evaluating the electrical equivalent parameters of a coil-wound saturistor will be applied for the modified rotor case. In this procedure, the magnetising force H_x and the hysteresis loss per unit volume per cycle p_x, which correspond to a specified maximum flux density B_x, are obtained from the static B–H curves of Alcomax III. Since the B–H curves available are at 50 Hz, the hysteresis loss per slot is given by

$$P_h = p_x \times \left(\text{volume of Alcomax III bar} \times \frac{f}{50}\right)$$
$$= I_b^2 R_s \quad . \tag{8}$$

I_b is the rms current flowing through the copper bar and is responsible for the

production of the magnetic field affecting the hard magnet bar at f Hz. The value of I_b is determined from the field configuration and slot dimensions as

$$I_b = H_x \cdot w_s + H_{\text{air}} \cdot w_a \quad . \tag{9}$$

The developed magnetic flux, assumed to have sinusoidal variation, will generate a back emf of an rms value of

$$E_{\text{rms}} = 4{\cdot}44\, \phi f \tag{10}$$

The effective impedance per slot of the hard magnet bar is given by

$$Z_s = \frac{4{\cdot}44\, \phi f}{I_b} \tag{11}$$

By varying B_x, the previous procedure enables the parameters R_s, Z_s and X_s of the Alcomax III bar to be computed at the given supply frequency f Hz.

STEADY-STATE PERFORMANCE OF THE MODIFIED MOTOR

The modified equivalent circuit per phase of an induction motor when Alcomax III bars are inserted above the copper bars of a squirrel cage rotor will be used for the derivation of the performance equations. This modified equivalent circuit per phase with rotor parameters referred to the stator is shown in Fig. 3, where

X_2' = referred (rotor leakage reactance excluding saturistor bar + rotor end-rings leakage reactance)
R_2' = referred (resistance of rotor copper bars + resistance of end-rings).

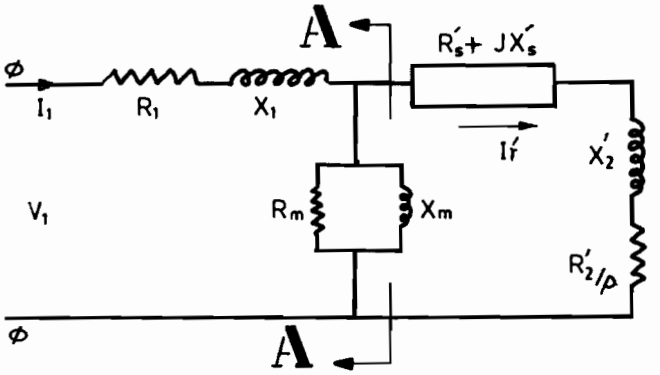

Fig. 3. The modified equivalent circuit per phase.

In the analysis to follow, the dependence of the saturistor parameters R_s and X_s on rotor current and frequency are considered in the same way as that developed by Dubey & De (1973). The circuit at the left of A–A in the modified equivalent circuit is replaced by its Thevenin equivalent as shown in Fig. 4. In using this circuit, it is assumed that voltage and current harmonics introduced by the saturistor are negligible. The following equation is derived from the above circuit

$$\left|\frac{E}{I'_r}\right|^2 = \left(R_1 + \frac{R'_2}{s} + R'_s\right)^2 + (X_1 + X'_2 + X'_s)^2 \tag{12}$$

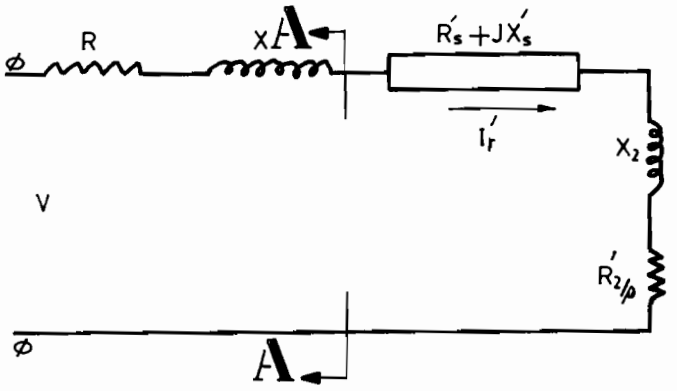

Fig. 4. Thevenin equivalent circuit of the motor.

The developed torque is given by

$$T = 3(I'_r)^2\left(R'_s + \frac{R'_2}{s}\right) \times \frac{7{\cdot}04}{\text{syn. speed}} \text{ lb-ft} \tag{13}$$

The stator input current per phase will be

$$I_1 = I'_r \frac{(R_m + R'_s + R'_2/s)^2 + (X_m + X'_s + X'_2)^2}{(R_m^2 + X_m^2)^{\frac{1}{2}}} \tag{14}$$

COMPUTATIONAL METHOD USED

Computations are commenced with a referred rotor current I'_r equal to an initial estimated value of the starting current required by the motor. The rotor slip is then calculated and the value of I'_r is adjusted iteratively until the condition of unity slip is reached. For each value of I'_r the corresponding parameters (R'_s and X'_s) of the saturistor bar are obtained by applying the subroutine SELECT which is a curve-reading program and is based on the straight line interpolation technique, supported by the two subroutines (ALCOM and VIND) to satisfy the required computations. A third subroutine (INPOLN) is also used for interpolation technique using the cord method. Motor performance is then computed at the resulted rotor current. The computation is repeated for lower values of I'_r. However, at each value of I'_r the corresponding value of slip is first computed before full performance is obtained. The computer flow diagram is shown in Fig. 5. The motor used in this investigation is a 3-phase squirrel cage induction motor with a 36-slot rotor. The stator parameters measured at 400 Hz supply are given by

$$R_1 = 0{\cdot}094\ \Omega$$

$$X_1 = 1{\cdot}1\ \Omega$$

$$X_m \quad 7{\cdot}95\ \Omega$$

$$R_m = 100\ \Omega$$

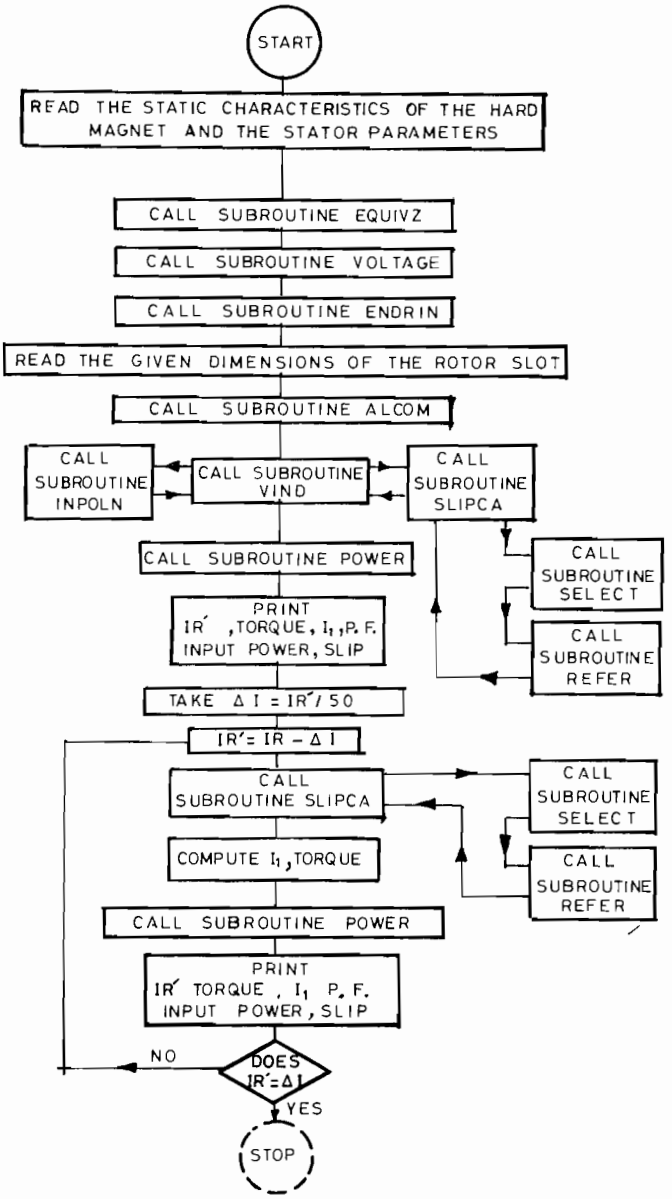

Fig. 5. The complete flow diagram.

The equivalent rotor parameters are computed from the dimensions and specifications given for the rotor (Alger 1965). The digital computer program was checked by computing the steady-state performance of an ordinary squirrel cage induction motor. These computed results are plotted in Fig. 6 together with those obtained from experimental tests. Comparison of the corresponding curves reveals that:

(i) good agreement is obtained with respect to input current;

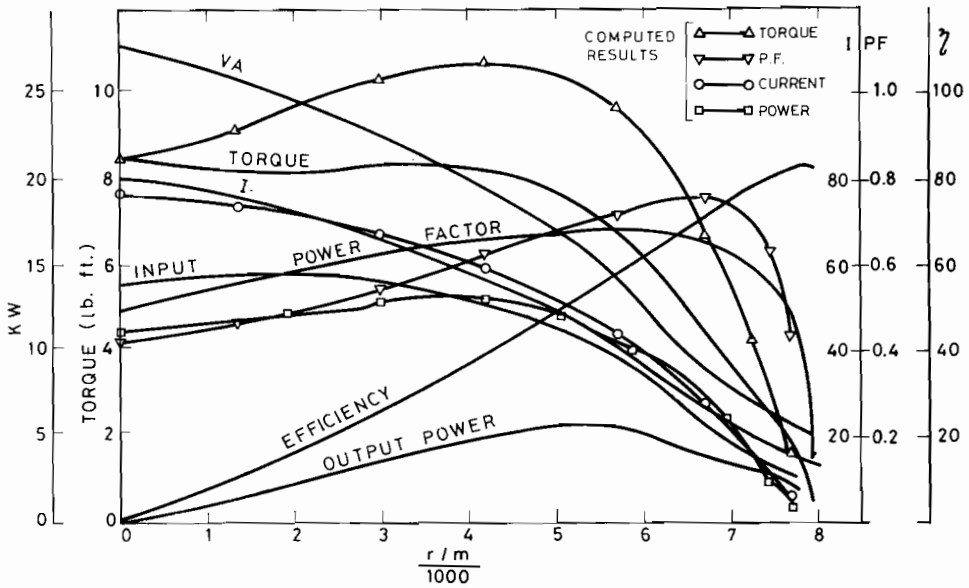

Fig. 6. Performance of non-saturistor motor.

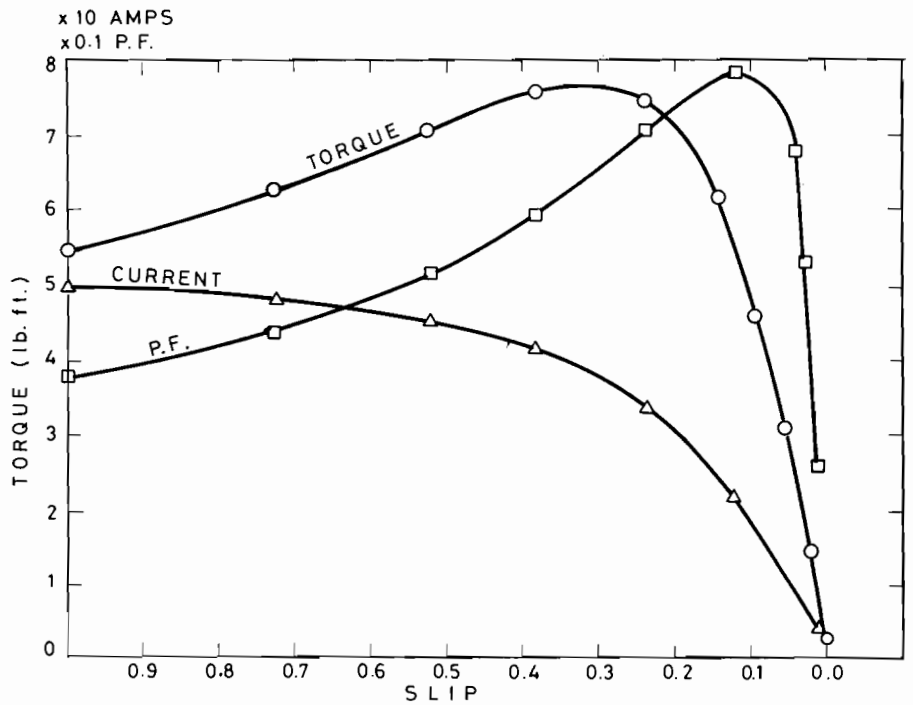

Fig. 7. Computed performance of near optimum design.

(ii) slip at peak value of torque is about the same;
(iii) starting torque is identical.

These indicate that the mathematical analysis and the corresponding digital simulation are satisfactory. The computer program is then used for computing the performance of the modified motor when Alcomax III bars are inserted in the slots of the rotor. The results obtained are presented in Fig. 7, which indicates the following advantages over the ordinary type of induction motor:

(i) The power factor of the modified motor is higher at full load conditions. This reflects the effect of hard magnetic material in the form of additional resistance to the rotor.
(ii) The input current of the modified motor is reduced to approximately half its value for ordinary type of motor. This reflects the additional impedance to the rotor circuit by the hard magnet bars.

CONCLUSIONS

The simulation results obtained in this work have justified the mathematical approach in dealing with a squirrel cage induction motor in which hard magnets have been introduced. It is clear that the eddy current effects can be neglected for small sizes of bars used at frequencies up to 400 Hz.

During starting, the saturistor bars exhibit higher resistance in comparison to the reactance of the rotor. In normal operation, the material will be of higher inductive reactance than its resistance. Further investigations are needed with different hard magnetic materials and different slot configuration for optimum performance.

ACKNOWLEDGEMENT

The author thanks the Research Council of the University of Kuwait for the facilities provided in connection with this work.

REFERENCES

Alger, P.L. 1965. The nature of induction machines. Gordon and Breach, London.

Alger, P.L., Angst, G. & Schweder, W.M. 1963. Saturistor and low starting current induction motor. AIEE Trans., PAS **82:** 291–98.

Dubey, G.K. & De, G.E. 1973. Saturistor control of induction motors. Proc. IEE **120:** 491–96.

Gunn, G.E. 1963. Improved starting performance on wound-rotor motors using saturistor. AIEE Trans., PAS **82:** 298–302.

Hick, C. 1974. Magnetic materials and their applications. Butterworths, London.

Sabir, S.A.Y. & Shepherd, W. 1974. Magnetic properties of Alcomax III with dynamic excitation. Proc. IEE **121:** 907–12.

Sabir, S.A.Y., Simmons, S. & Shepherd, W. 1975. Design of saturistors for induction motor speed control. IEEE Trans. on Industry Applications **5:** 150–54.

Shepherd, W., Gaskell, H. & Rashid, P. 1974. Variation with specimen size of some properties of Alcomax III at 50 Hz excitation. IEEE Trans., Mag. **10:** 50–54.

(Received 30 April 1983, revised 16 November 1983)

استخدام المواد ذات المغنطة الدائمة في تحسين أداء المحركات الكهربائية

محمد حسن سلامه
قسم الهندسة الكهربائية بجامعة الكويت

خلاصة

في هذا البحث تم تمثيل المواد ذات المغنطة الدائمة والتي تعطي فقدا اعصاريا كبيرا عند تعرضها لمجال كهربي متردد ، بدائرة كهربائية .

وعند استخدام هذه المواد على صورة قضبان ذات أبعاد محددة في فجوات العضو الدوار لمحرك تأثيري ، تم دراسة تأثير هذه القضبان باضافة مكونات الدائرة الكهربائية التي تمثلها إلى الدائرة الكهربائية المكافئة للمحرك التأثيري . وكان الغرض من زرع هذه القضبان هو الحصول على أداء أفضل للمحرك ، ومن أجل هذا تم تصميم برنامج على الحاسب الالكتروني لتحقيق المتطلبات السابقة .